Carbon – Science and Technology

ISSN 0974 – 0546

http://www.applied-science-innovations.com

ARTICLE Received : 15/07/2013, Accepted : 03/09/2013

(Special Section on Advanced (Non-Carbon) Materials)

Effect of heat treatment on $Mn_xZn_{(1-x)}Fe_2O_4$ nanoparticles prepared by mechano-chemical method using metal oxides

G. V. S. Kundaikar

Department of Physics, Goa University, Taleigio, Goa – 403 206, India.

ABSTRACT : Nanoparticles of $Mn_xZn_{(1-x)}Fe_2O_4$ where x = 0.625, 0.65 and 0.675 with grain size ranging between 15 nm – 25 nm were prepared by novel technique employing low temperature auto-combustion. XRD, IR and TEM techniques were used to obtain structural and morphological characterizations. XRD and IR spectra confirmed the formation of spinel structure. Stoichiometry of the samples was confirmed with EDS spectral analysis. Nanocrystalline nature of the sample was observed in HRTEM of the samples and formation of the nanoparticles was confirmed by measuring crystallite size using XRD pattern and TEM. Magnetic properties of the nanosample obtained with VSM give values ranging between 45.25 – 50.92 emu/gm; 0.0009 - 0.0055 Tesla, and 2.77 – 9.4 emu/gm for saturation magnetization, coercivity and retentivity, respectively. Curie temperature values ranging between 380 ^{0}C – 540 ^{0}C were obtained for the powdered samples. Magnetic measurements like saturation magnetization Ms, coercivity Hc, and retentivity Mr, carried out on the bulk samples obtained at 900 ^{0}C show that the samples lose the magnetic properties and behaved as paramagnetic material.

Keywords : Nanoparticle, Saturation Magnetization, Coercivity, Retentivity, A. C. Suceptibility.

INTRODUCTION : Manganese-zinc ferrites belong to the group of soft ferrite materials. Mn-Zn spinel ferrite nanoparticles are extensively used in variety of applications like microwave devices, computer memory chip, magnetic recording media, transformer cores and rod antennas etc **[1].** Targeted drug delivery systems and hyperthermeia **[2]** are some new applications in medical sciences**.** A remarkable variation in magnetic properties of these nanoparticles is attributed to pinning of spins at particle surface, or the presence of a dead layer around the magnetic core material. Interparticle interactions are another factor controlling anomalous behavior of these nanoparticles **[3]**. Magnetic behavior is largely affected by numerous imperfections in the material. Imperfections like surface spin canting, lattice distortions at the surface of the particles **[4]** play a major role in deciding the magnetic properties of the material as the surface to volume ratio is large in this type of materials. The contribution arising from surface is large in the nanomaterials. This indeed makes the particle size very important parameter as the same can change the material properties drastically due to changing surface to volume ratio. The mechanism governing the magnetic super exchange phenomena is well known **[5]** in these materials.

The present research was undertaken with a dual objective of preparing nanoparticles using metal oxides and to study the properties of bulk material produced from these nanoparticles. The basic goal of preparing nanoparticle $Mn_xZn_{(1-x)}Fe_2O_4$ material at low temperature using metal oxides was achieved by adopting mechano-chemical autocombustion method. The bulk material was obtained from these

nanoparticles by sintering the compressed nanoparticles in nitrogen atmosphere at different temperatures. Since the solid state reaction with metal oxides is initiated at high temperatures beyond 900 ^{o}C it was necessary to bring down the reaction temperature by adopting a suitable procedure or an appropriate technique. The reaction temperature being a function of activation energy it was felt necessary to bring down the activation energy of the solid state system by mechanical ball milling. Thus the activation energy of reaction was lowered by downsizing the particles in the mixture of metal oxides and by addition of appropriate ligand. Downsizing of the constituents of the mixture brings the reactant particles close together, increases the surface area to volume ratio of the reactants, increases reactivity and speed of chemical reaction thus lowering the activation energy. Reduction in activation energy makes the reactants react at lower temperature to produce the desired material.

EXPERIMENTAL : Starting material in the form of metal oxides was taken in desired proportion, ball milled by using Acmas Technocracy Weiber Ball Mill Model (Acm-82303), at 80 rpm for 10 hours. This mixture was treated with calculated amount of ligand and thoroughly homogenized to obtain a thick paste. The paste was dried using conventional heating till it ignites to produce the sample. Sample yield was calculated and titrimetric chemical analysis was carried out on the samples to confirm the composition. X-ray diffraction patterns were recorded on the Rigaku diffractrometer using Cu-$K_{\acute{a}}$ radiation and scanning angle range of 20 to 80 degrees. Lattice constant, and grain size values were calculated using XRD data. IR absorption spectra were recorded on Shimadzu FTIR 8900 spectrometer in the range of 350 cm^{-1} to 4000 cm^{-1}. EDAX spectra were recorded on JEOL Model 840 (SEM) for stoichiometry confirmation. Transmission electron micrograph (TEM) of the sample was taken on FEI TECNAI 200KV HRTEM. The fine powdered samples were then pressed into pellets of dimension 1 cm diameter and thickness 3 mm, by applying pressure of $9.554\mathbf{x}10^{8}$ Newton/m^2 for duration of 10 minutes**.** The pellets were sintered at 900 ^{0}C for four hours in nitrogen atmosphere to obtain the bulk sample. Magnetic properties of the samples were recorded on Vibrating Sample Magnetometer (VSM) by employing OXFORD Instruments, UK. Specific magnetization measurements as a function of temperature of the nanosamples were carried out on standard high pulse field AC susceptibility measuring apparatus.

RESULT AND DISCUSSION :

CHEMICAL ANALYSIS : The comparison of theoretically calculated percentage yield with regard to the quantity of raw material taken and experimental yield confirmed that the desired mixed oxide material is formed by the method formulated. Estimated values of Mn, Zn and Fe from EDS analysis are in good agreement with the theoretical values, thus confirming the preservation of stoichiometry **[6].**

Table (1) : Theoretical and experimental percentage yield for $Mn_xZn_{(1-x)}Fe_2O_4$ material.

Composition $\mathbf{Mn_xZn_{(1-x)}Fe_2O_4}$	**Theoretical Yield**	**Experimental Yield**	**% Yield**
X=0.625	**9.3818**	**9.3217**	**99.36**
X=0.65	**9.3713**	**9.3469**	**99.74**
X=0.675	**9.3609**	**9.3197**	**99.56**

Table (2) : EDS data for $Mn_{0.65}Zn_{0.35}Fe_2O_4$ sample

Element	Wt. %	Atomic%
O K	30.75	63.91
Mn K	14.96	8.05
Fe K	45.05	23.86
Zn K	9.24	4.18
Totals	100.0	

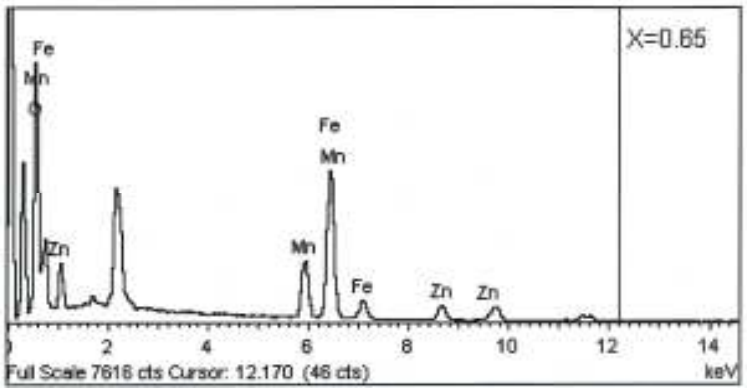

Figure (1) : EDS spectrum of $Mn_{0.65}Zn_{0.35}Fe_2O_4$ sample

Table (3) : Estimated percentage error of the elements Mn, Zn and Fe in the nanosample $Mn_xZn_{(1-x)}Fe_2O_4$.

	Mn		Zn		Fe	
Sample	EDAX values	% error	EDAX values	% error	EDAX values	% error
$Mn_{0.625}Zn_{0.375}Fe_2O_4$	0.615	1.60	0.3698	2.67	1.88	6.0
$Mn_{0.65}Zn_{0.35}Fe_2O_4$	0.6378	1.88	0.3311	5.4	1.89	5.5
$Mn_{0.675}Zn_{0.325}Fe_2O_4$	0.7220	-6.9	0.327	-0.62	2.09	-4.5

Slight deviation of Mn, Zn, and Fe contents in the nanosamples [Table 3] calculated from EDS data seem to be reasonable.

CHARACTERIZATION :

X-ray Diffraction (XRD) Analysis :

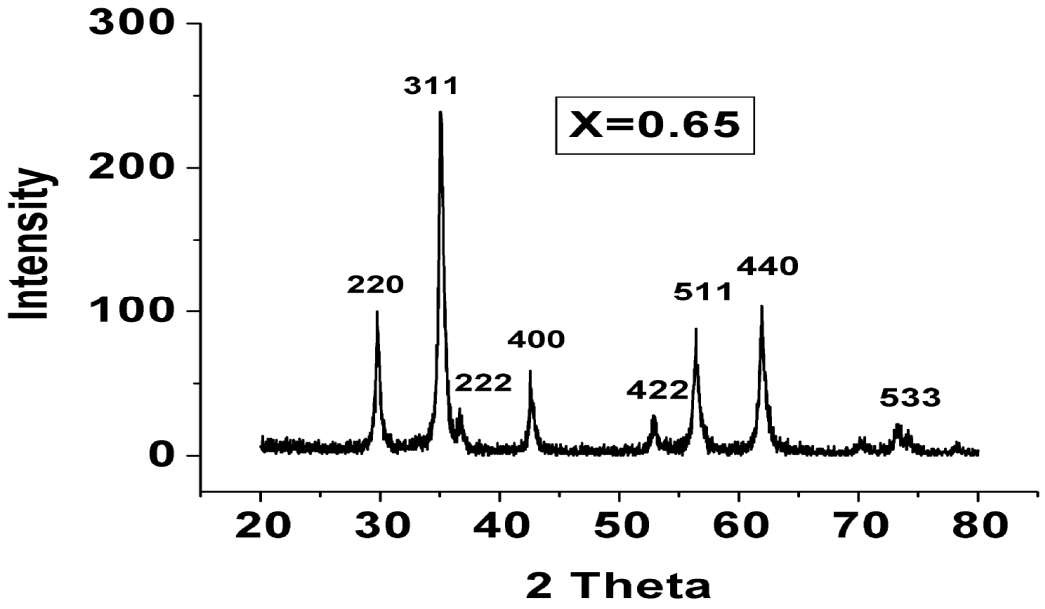

Figure (2) : XRD of $Mn_{0.65}Zn_{0.35}Fe_2O_4$ sample.

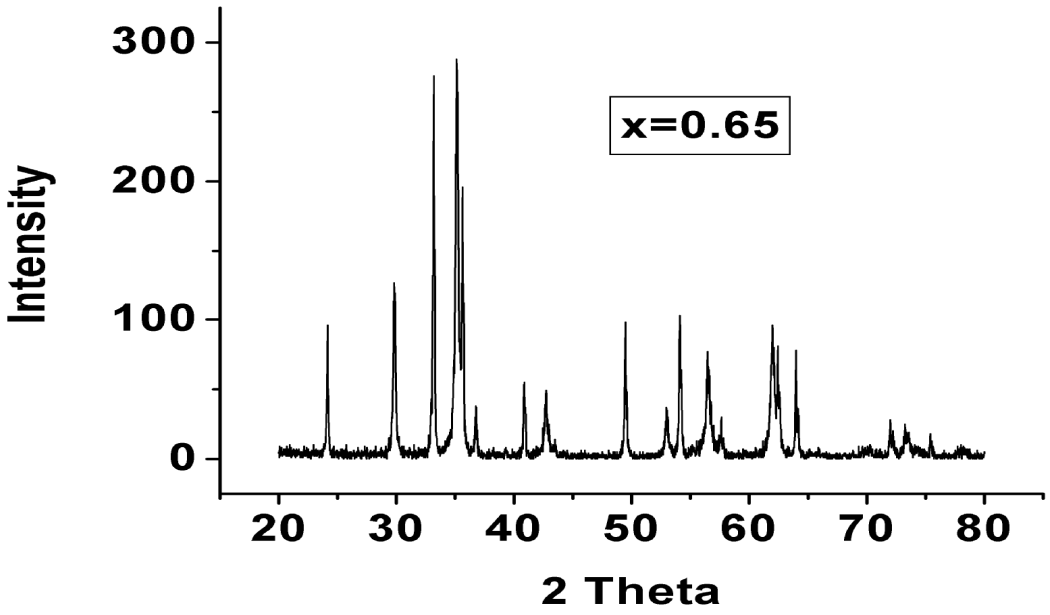

Figure (3) : XRD of $Mn_{0.65}Zn_{0.35}Fe_2O_4$ sample sintered at 900^oC

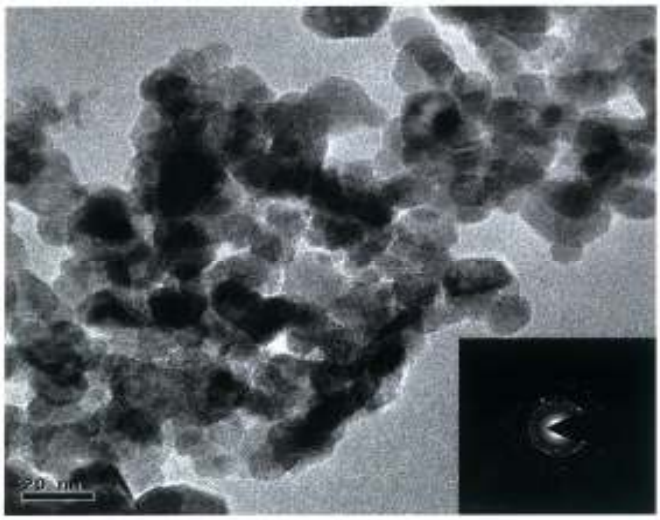

Figure (4) : HRTEM micrograph of $Mn_{0.65}Zn_{0.35}Fe_2O_4$ sample.

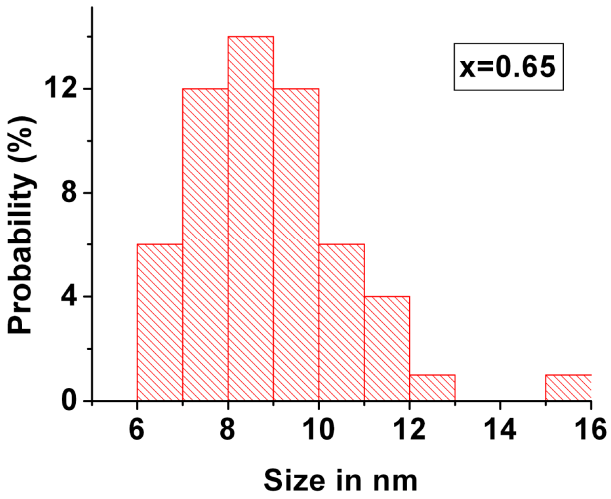

Figure (5) : Particle Size Histogram of $Mn_{0.65}Zn_{0.35}Fe_2O_4$ sample

Table (4) : Particle size and lattice constant for $Mn_xZn_{(1-x)}Fe_2O_4$ sample.

Concentration of Mn x	Lattice Constant "a" A°	Particle Size (Scherrer's Formula) "t" nm	Average particle size 't' (by using TEM) in nm
0.625	8.4396	12.50	11.13(2.17)
0.65	8.4502	17.55	8.9(1.71)
0.675	8.4622	16.92	13.66(2.64)

Figure (2) shows the X–ray diffraction pattern for as prepared $Mn_{0.65}Zn_{0.35}Fe_2O_4$ sample. Similar patterns were also obtained for other nanosamples. The observed diffraction patterns are identical to those of standard pattern of Mn-Zn ferrite with no extra peaks, thereby indicating all the samples are single phase spinel structure **[7].** The lattice constant determined using X-ray diffraction pattern increases with increasing Mn concentration and is found to be in good agreement with reported data **[3, 8]**. This increase is due to the replacement of Zn cations having a smaller ionic radius by Mn cations having a larger one **[3]**. Particle size calculated from X- ray by peak broadening method, is in the range of 12 nm to 17 nm. High Resolution Microscopy has also been used to confirm the nanoparticle size and to determine the particle size distribution. The size distribution has been determined from the histogram obtained by measuring the size of around sixty individual particles using image J software. The histogram of sample $Mn_{0.65}Zn_{0.35}Fe_2O_4$ (Figure 4 & 5) shows that the maximum size distribution is in the range of 7 nm to 10 nm. Also the particle size values observed from HRTEM (8 nm to 14 nm) (Table 4) are comparable to those obtained from the X- ray peak broadening technique.

INFRA RED SPECTROSCOPY (IR) : Infrared absorption spectra of the samples under investigation show two significant absorption bands revealing the formation of single phase cubic spinel.

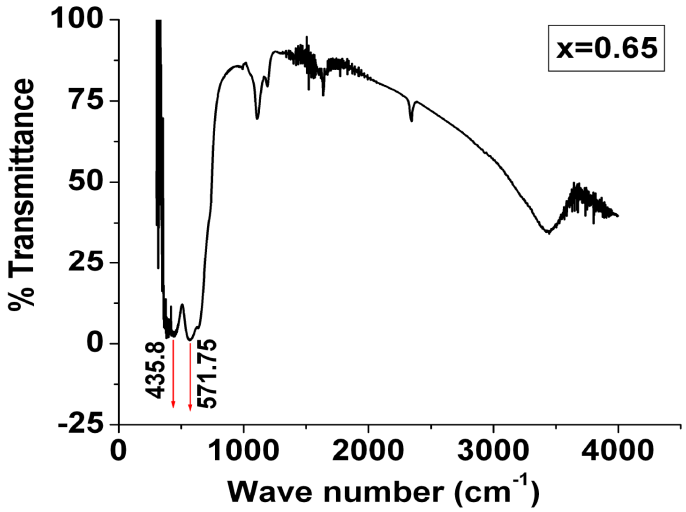

Figure (6) : IR absorption spectrum of $Mn_{0.65}Zn_{0.35}Fe_2O_4$.

The first absorption band, observed at about 550 cm^{-1} to 600 cm^{-1}, is attributed to the tetrahedral site, whereas the second band observed at 330 cm^{-1} to 425 cm^{-1} is assigned to the octahedral group complexes **[9]**. The positions of absorption bands are compositional dependent, which could be attributed to the variation in cation oxygen bond distances **[9]**.

MAGNETIC MEASUREMENT :

VSM : Hysteresis curves of nanosamples $Mn_xZn_{(1-x)}Fe_2O_4$ (x= 0.625, 0.65, 0.675) obtained at room temperature are shown in the Figure 7(a, b, c). The saturation magnetization Ms for the bulk samples is found to show a very unusual pattern. The bulk samples obtained at 900 ^oC surprisingly show substantial quenching of magnetic moment. However the samples regain magnetization when sintered at higher temperatures (Figure 8).

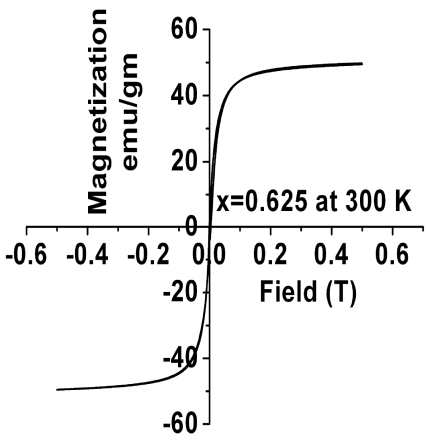

Figure (7a)

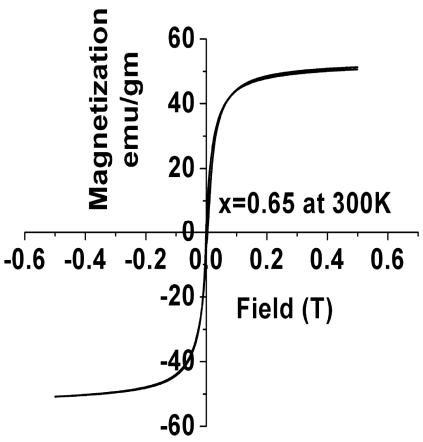

Figure (7b)

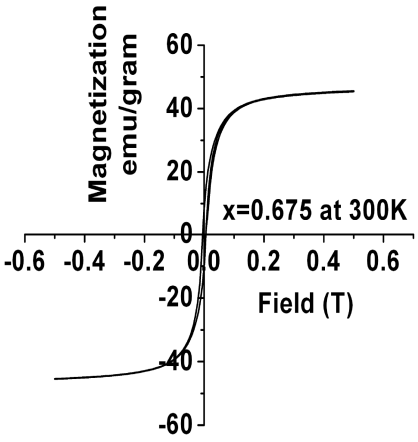

Figure (7c)

Figure (7) : Hystersis curve of (a) $Mn_{0.625}Zn_{0.375}Fe_2O_4$ (b) $Mn_{0.65}Zn_{0.35}Fe_2O_4$ (c) $Mn_{0.675}Zn_{0.325}Fe_2O_4$ obtained by using VSM

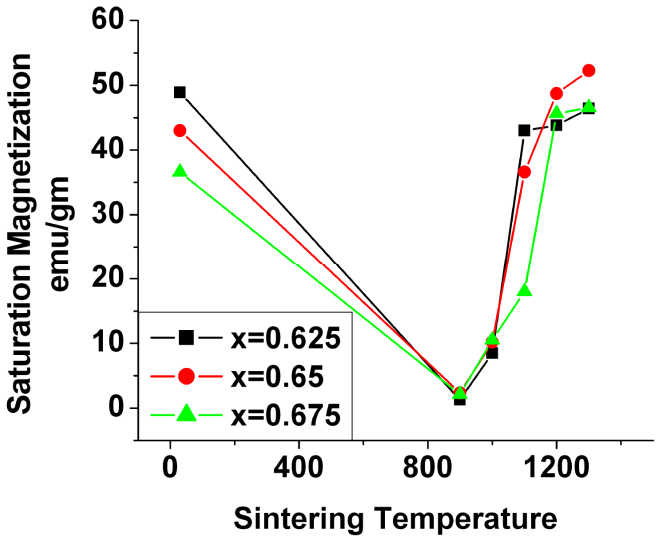

Figure (8) : Variation of Saturation Magnetization with sintering temperature of $Mn_xZn_{1-x}Fe_2O_4$ (x=0.6, 0.65, 0.675)

It is reported **[10]** that when Mn-Zn ferrite is sintered in air, Mn^{+2} oxidizes to Mn^{+3} at temperature above 200 ^{0}C and below 900 ^{0}C. Above 900 ^{0}C Mn^{+2} becomes stable again and MnZn ferrite starts to reform. It was clearly shown in the literature that Mn-Zn ferrite decomposes to paramagnetic $ZnFe_2O_4$ and antiferromagnetic Fe_2O_3 and Mn_2O_3 which is the reason for diminishing the magnetization at 800 ^{0}C **[10]**. Present investigation has revealed that nanoparticle samples sintered at 900 ^{o}C in nitrogen atmosphere exhibits quenching of magnetic moments to the extent of 97 to 99 %. This is due to the decomposition of the sample and break down of the structure with the formation of the products of the type Fe_2O_3 with major peak at $2\theta = 33^o$, along with Mn_2O_3 and ZnO which is responsible for the diminishing of magnetization **[11]** as it is confirmed from the XRD of the bulk sample (Figure 3).

The other possibility may be the formation of magnetically dead layer at the surface of the nanoparticles. This can happen due to partial evaporation of Zn from the surface of the nanoparticles. This fact can give rise to lattice distortion in the sample sintered at 900 ^{o}C. As the sintering temperature is increased above 900 ^{0}C, it is observed that, all the samples show an increase in saturation magnetization, which increases with corresponding rise in sintering temperature. This could be attributed to increase in particle size, crystallinity, improvements on microstructure. Also this could be due to decomposition of nonmagnetic Fe_2O_3 and Mn_2O_3 **[11]** formed in the sample as a result of previous sintering process at lower temperature. Magnetic parameters obtained for nano and bulk sample at 900 ^{0}C are presented in (Table 5 and 6).

Table (5) : Saturation magnetization, retentivity, squareness and coercivity values for Mn-Zn ferrite nano samples by using VSM at room temperature.

Mn content (x)	**Saturation Magnetization emu/gm**	**Coercivity Tesla**	**Retentivity Mr emu/gm**	**Squarness Mr/Ms**
0.625	**49.66**	**0.0009**	**2.77**	**0.557**
0.65	**50.92**	**0.0014**	**4.31**	**0.0846**
0.675	**45.25**	**0.055**	**9.4**	**0.2**

Table (6) : Saturation magnetization, retentivity, squareness and coercivity values of bulk Mn-Zn ferrite samples sintered at 900 ^{0}C.

I. II. COCNCENTRATION OF MN **(x)**	**Saturation Magnetization** III. EMU/GM IV.	**Coercivity (Hc) in Oersted**	V. **Retentivity(Mr)** VI. EMU/GM	**Decrease Ms**
VII. X=0.625	VIII. 1.39	IX. 85.83	X. 1.69	**97.04%**
XI. X=0.65	XII. 1.69	XIII. 83.61	XIV. 0.83	**96.75%**
XV. X=0.675	XVI. 0.59	XVII. 577	XVIII. 3.26	**98.84%**

AC SUSCEPTIBILITY : AC susceptibility curves shown in Figure (9) or nanoparticle samples indicate that the samples are mixtures of single domain and multi domain particles. The sample with x= 0.625, 0.65 and 0.675 exhibit a narrow multidomain (MD) character in addition to single domain (SD) behavior **[12]**. However, the quantity of MD grains in the samples appears to depend on Mn concentration in the sample.

The samples with x=0.65 and 0.675 appear to have more grains with MD then samples with x=0.625 where SD character is more predominant. AC susceptibility trend for all the nanosamples exhibit ferrimagnetic behavior **[13, 14]**. The Curie Temperature (T_c) increases with Mn concentration in the samples. The Curie temperature (T_c) is 387 ^oC and 394 ^oC for nanosample $Mn_{0.625}Zn_{0.375}Fe_2O_4$ and $Mn_{0.65}Zn_{0.35}Fe_2O_4$, respectively, which increases to 536 ^oC for $Mn_{0.675}Zn_{0.325}Fe_2O_4$. High T_c indicates the presence of metastable state in the samples **[3]**.

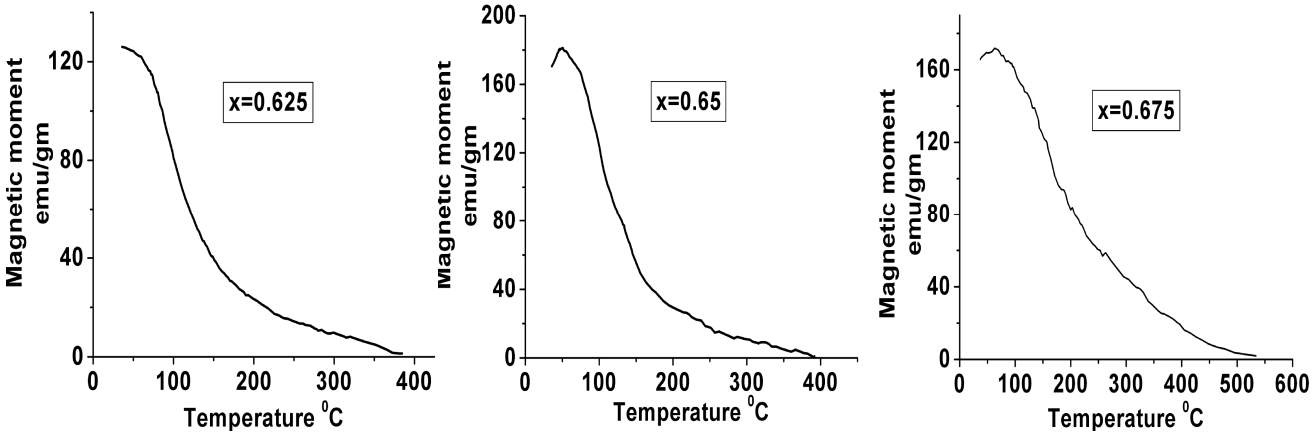

Figure (a) Figure(b) Figure(c)

Figure (9) : AC Sussceptibility curves of nanosample $Mn_xZn_{(1-x)}Fe_2O_4$ for (a) x=0.625, (b) x= 0.65, and (c) x= 0.675

CONCLUSIONS : Nanoparticle ferrite samples are prepared by the method which makes use of individual metal oxide powders as starting material. The nanoparticles showed narrow hysteresis loop. Particle size of as prepared samples are in the range of 12 nm to 18 nm. AC susceptibility of $Mn_{0.625}Zn_{0.375}Fe_2O_4$ decreases almost exponentially with increase in temperature indicating the presence of more single domain particles in the samples. However, the AC susceptibility for $Mn_{0.65}Zn_{0.35}Fe_2O_4$ and $Mn_{0.675}Zn_{0.325}Fe_2O_4$ samples initially show rise followed by exponential fall. This indicates that the samples contain some multidomain particles which are very few in numbers. The nanosamples show high Curie temperature values. Hystersis and AC susceptibility curves exhibits superparamagnetic behavior of the particles. It was observed that saturation magnetization is drastically reduced for the bulk samples (900 ^0C). However the samples regain the magnetization at higher sintering temperatures.

ACKNOWLEDGEMENT : Authors acknowledge Dr. Ayub, Senior Scientist, Department of Material Science TIFR Mumbai, for his help in TEM measurement. We also like to express our gratitude to Dr. Nigam, Department of Condensed Matter TIFR Mumbai for his help in VSM measurements.

REFERENCES :

1. Uzma Ghazanfar, S. A. Siddiqi, G. Abbas, Structural analysis of the Mn–Zn ferrites using XRD technique, Materials Science and Engineering B 118 (2005) 84 - 86.
2. M. A. Willard, L. K. Kurihara1, E. E. Carpenter, S. Calvin and V. G. Harris, Chemically prepared magnetic nanoparticles, International Materials Reviews 49 (2004) 125 – 170.
3. Chandana Rath, S. Anand, R. P. K. Sahu, S. D. Kulkarni, S. K. Date and N. C. Mishra, Dependence on cation distribution of particle size, lattice parameter, and magnetic properties in nanosize Mn–Zn ferrite, Journal of Applied Physics, Vol. 91 No. 415, (2002).

4. D. Santhosh Kumar, K. Chandra Mouli, International Journal of Nanotechnology and Applications, ISSN 0973-631X Volume 4,No. 1(2010), pp.51-59.
5. B. Vishwanathan, V. R. K. Murthy, Ferrite Materials, Science and Technology, Narosa Publishing House, 1990.
6. S. Son, R. Swaminathan and M. E. McHenry, Structure and magnetic properties of rf thermally plasma synthesized Mn and Mn–Zn ferrite nanoparticles, J. of Applied Physics 93/10 (2003).
7. B. D. Culity, 1959, Elements of X-ray diffraction, 132.
8. R. G. Welch, J. Neamtu, M. S. Rogalski, S. B. Palmer, Polycrystalline MnZn ferrite films prepared by pulsed laser deposition, Materials Letters 29 (1996) 199 – 203.
9. B. P. Ladgaonkar, C. B. Kolekar, A. S. Vaingankar, Indian Academy of Science, Infrared absorption spectroscopic study of Nd^{3+}substituted Zn-Mg ferrite, Bull. Meter. Sci. Vol. 25, No.4, (2002) 351 - 354.
10. Rozman M. and Drofenic M., Hydrothermal synthesis of Manganese Zinc Ferrite, J. Am. Ceram. Soc. 78 (1995) 2449 – 55.
11. Ping Hu, Hai-bo Yang, De- an Pan, Hua Wang, Jian –jun tian, Shen-gen Zhang, Xin- feng Wang, Alex A. Volinsky, Heat treatment effects on microstructure and magnetic properties of Mn-Zn ferrite powders, Journal of Magnetism and Magnetic Materials 322 (2010) 173 - 177.
12. N. D. Chaudhari, R. C. Kambale, D. N. Bhosale, S. S. Suryavanshi, S. R. Sawant, Thermal hysteresis and domain states in Ni–Zn ferrites synthesized by oxalate precursor method, Journal of Magnetism and Magnetic Materials 322/14 (2010) 1999 - 2005.
13. R. V. Upadhyay., S. N. Rao and R. G. Kulkarni "Yafet-Kittel type of magnetic ordering in Mg-Cd ferrites, Materials Letters 3 (1985) 273 – 277.
14. J. Hopkinson, Magnetic and other physical properties of iron at a high temperature, Philos. Trans. R. Soc. (London) 180 (1889) 443.